Inter-comparisons of Daily Sea Surface Temperature Data and In-Situ Temperatures at Korean Coastal Regions

Kyung-Ae Park[1)], Hye-Jin Woo[1)], Hee-Young Kim[2)]

1) Dep. of Earth Science Education, Seoul National University, Seoul, Korea, Email: kapark@snu.ac.kr

2) Dep. of Science Education, Seoul National University, Seoul, Korea.

Abstract

This study presents results from the validation of seven global blended sea surface temperature (SST) analyses using the in-situ temperature measured from the coastal wave buoy and inter-comparison of them in the seas around the Korean Peninsula from 2014 to 2018: OSTIA (Operational SST and Sea Ice Analysis) CMC (Canadian Meteorological Centre) analysis, OISST (Optimum Interpolation SST), REMSS (Remote Sensing System) analysis, MURSST (Multi-scale Ultra-high Resolution SST), and MGDSST (Merged Satellite and In situ Data Global Daily SST). Overall, the root-mean square error of each analysis for the in-situ measurements was relatively high at a range from 1.27°C (OSTIA) to 1.74°C (REMSS). All analyses had warm biases over 0.29°C, which were distinctive in the southwestern coastal region of the Korean peninsula with remarkable SST cooling due to strong tidal currents in summer. In the comparison of temporal variability, most analyses revealed low coherency (< 0.5) in the period shorter than 10 days. The SST analyses have been compared against each other by investigating the spatial distributions of RMSE and bias errors. While most SST analyses tended to show good agreement in the open ocean, the differences had tendency to be amplified at the coastal regions and frontal regions. We discussed potential factors that cause the errors of SST analyses at the coastal regions by presenting the effects induced by grid sizes, distance from the coast, energy spectra, wavelet coherence, and thermal fronts in the marginal seas of the Northwest Pacific.

Introduction

SST analysis has been produced by institutions worldwide for various purposes and quality assessments of each product have been performed, both by comparison with in-situ measurements and by inter-comparison between SST analyses across global oceans. In contrast, validation and comparison of SST products in regional areas has been reported as insufficient, and there has been even less attention given to the coastal regions, despite its essential importance.

Study Area

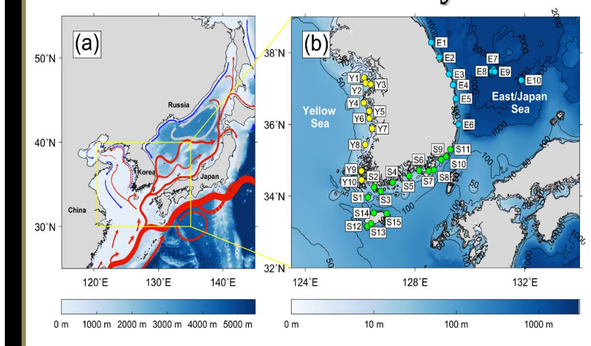

Fig. (a) Currents in the study area, where the color blue represents water depth; (b) enlarged bathymetry map for the seas around the Korean Peninsula. Blue, green, and yellow dots and black text represent the location and symbol of the coastal wave buoys of Korean Meteorological Administration.

Objectives

(1) to evaluate the accuracies of the SST products applicable to the seas around the Korean Peninsula;

(2) to analyze the error characteristics of the SST products using in-situ temperature data measured by the coastal wave buoys operated by the Korea Meteorological Administration (KMA);

(3) to compare SSTs among the databases in the Northwest Pacific;

(4) to identify the strength and weakness of each SST analysis database;

(5) to provide information on the SST databases in the coastal regions.

Data and Methods

SST analyses

Table. Information on the sea surface temperature (SST) analyses used in this study, where the input data were investigated based on the SST analysis information on January 1, 2014, or on information from the respective database website.

Name	Period	Spatial resolution (°)	Input data			Agency
			IR	MW	In-situ	
OSTIA	**Jan 2007 – present**	**0.05**	**AVHRR, IASI, SEVIRI, GOES13 Imager**	**TMI**	**GTS**	**Met Office**
CMC analysis	Sep 1991 – present	0.2 (~2017) 0.1 (2016~)	AVHRR	Windsat	GTS	CMC
OISST	Sep 1981 – present	0.25	AVHRR	-	GTS	NCEI/ NOAA
REMSS analysis	**Jun 2002 – present**	**0.09**	**MODIS**	**AMSR2, TMI, Windsat**	**-**	**REMSS**
MURSST	**Jun 2002 – present**	**0.01**	**AVHRR, MODIS**	**AMSR2**	**iQUAM**	**JPL/ NASA**
MGDSST	**Jan 1982 – present**	**0.25**	**AVHRR**	**AMSR-E, Windsat, AMSR2**	**GTS**	**JMA**
Blended SST	Sep 2002 – present	0.05	AVHRR, JAMI, GOES Imager	-	-	NESDIS/ NOAA

- The data used in this study covered the period 2014–2018.

In-situ Measurements

- During the study period, water temperatures were measured at 35 coastal wave buoys located around the Korean Peninsula, with 10 of these located in the EJS, 15 buoys in the southern region, and 10 buoys in the Yellow Sea.
- The precision and temporal resolution of their water temperature measurements were 0.1 K and 1 hour, respectively.

Error Analysis Methodology

$$Bias = \frac{1}{N}\sum_{i=1}^{N}(x_i - y_i), \qquad RMSE = \sqrt{\frac{1}{N}\sum_{i=1}^{N}(x_i - y_i)^2},$$

$$E_{com} = \sqrt{RMSE^2 + Bias^2},$$

where x_i represents the SST analysis, y_i stands for the buoy temperature, and $\bar{x}$ and $\bar{y}$ represent the average values of the SST analysis and buoy temperature, respectively. N represents the number of the data

Results

Spatial Distribution of SST analyses

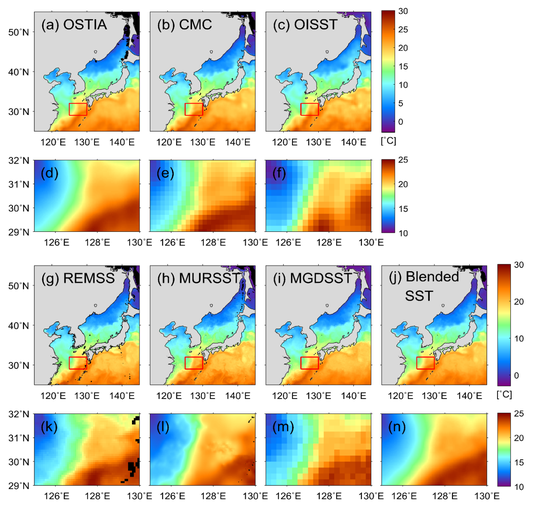

Fig. Spatial distribution of sea surface temperatures—(a) OSTIA; (b) CMC analysis; (c) OISST; (d–f) enlarged SST data for the red box in (a–c); (g) REMSS analysis; (h) MURSST; (i) MGDSST; (j) Blended SST; and (k–n) enlarged SST data for the red box in (g–j).

Accuracy Assessments of SST Analyses

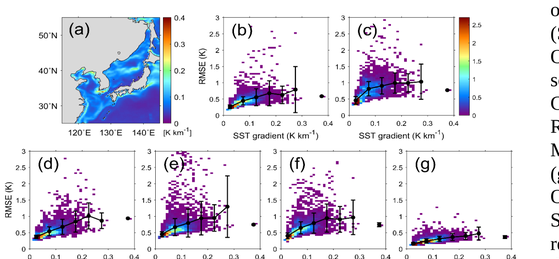

Fig. Comparison between sea surface temperature (SST) analyses and in-situ temperatures from coastal wave buoys—(a) OSTIA; (b) CMC analysis; (c) OISST; (d) REMSS analysis; (e) MURSST; (f) MGDSST; and (g) Blended SST.

Spatial Distribution of SST Errors

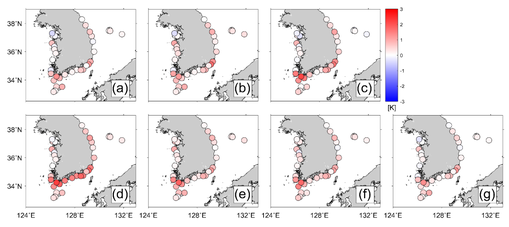

Fig. Spatial distribution of the bias errors of SST analysis at the location of the coastal wave buoys.

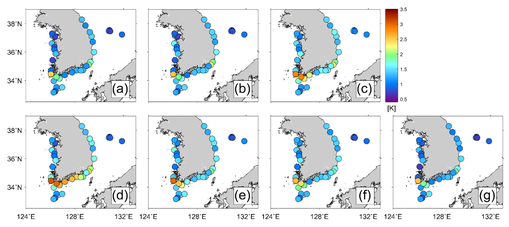

Fig. Spatial distribution of the RMSEs of SST analysis at the location of the coastal wave buoys.

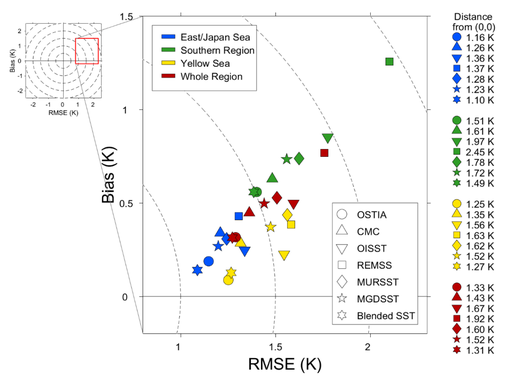

Fig. Scatter plot of RMSE and bias in SST analyses in the East/Japan Sea, southern region of the Korean Peninsula, Yellow Sea, and for the region as a whole. Dashed contours represent the constant value of the distances from the zero bias and zero RMSE.

Comparison of Wavelet Coherence

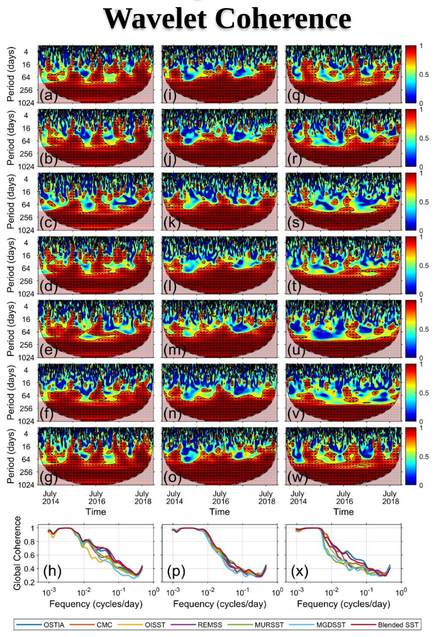

Fig. Wavelet coherence between in-situ temperature and (a) OSTIA, (b) CMC analysis, (c) OISST, (d) REMSS analysis, (e) MURSST, (f) MGDSST, and (g) Blended SST. (h) Global coherence at the location of the E4 buoy; (i)–(p) and (q)–(x) are the same as (a)–(h), but at the locations of S2 and Y10, respectively.

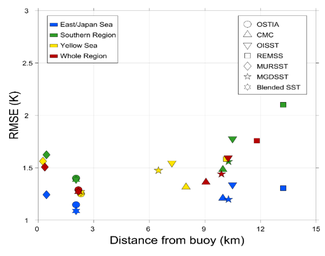

Fig. Scatter plot of RMSE of SST analysis as a function of distance between the center of grid cell of SST analyses and the position of coastal wave buoys.

Inter-comparison of the SST Products

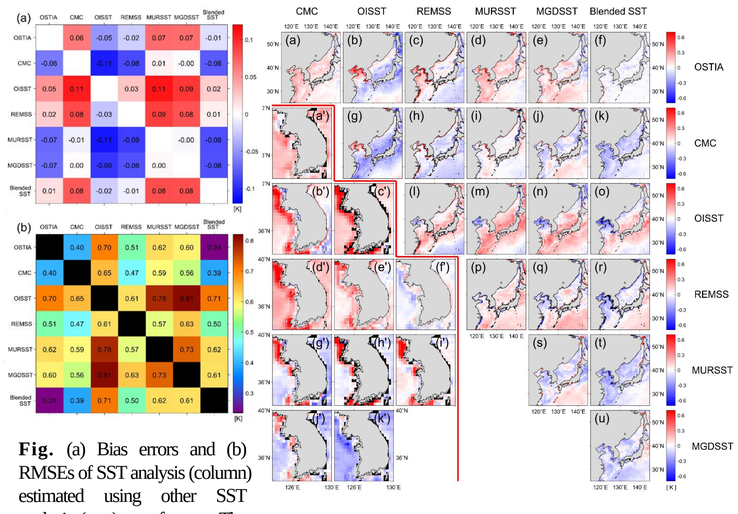

Fig. (a) Bias errors and (b) RMSEs of SST analysis (column) estimated using other SST analysis (row) as reference. The errors were obtained for SST differences by subtracting one SST product on the left side from the other SST product listed at the top.

- For inter-comparison between the SST products, spatial averaged RMS difference and bias between each SST analysis were estimated for the entire marginal sea region of the Northwest Pacific (25-55°N, 115-145°E).

Fig. Spatial distribution of bias of (a) CMC analysis, (b) OISST, (c) REMSS analysis, (d) MURSST, (e) MGDSST, and (f) Blended SST for the OSTIA; (g) OISST, (h) REMSS analysis, (i) MURSST, (j) MGDSST, and (k) Blended SST for the CMC analysis; (l) REMSS analysis, (m) MURSST, (n) MGDSST, and (o) Blended SST for the OISST; (p) MURSST, (q) MGDSST, and (r) Blended SST for the REMSS analysis; (s) MGDSST and (t) Blended SST for the MURSST; and (u) Blended SST for the MGDSST. (a'–k') are enlarged from (a–k), respectively.

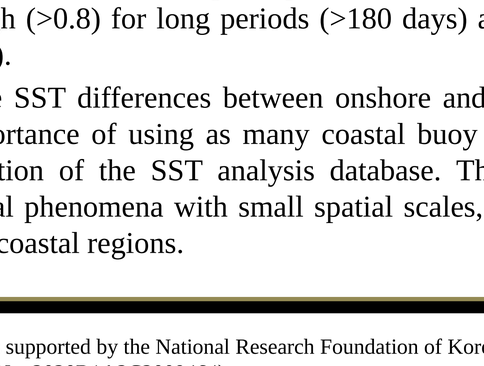

Fig. Spatial distribution of RMSE of (a) CMC analysis, (b) OISST, (c) REMSS analysis, (d) MURSST, (e) MGDSST, and (f) Blended SST for the OSTIA; (g) OISST, (h) REMSS analysis, (i) MURSST, (j) MGDSST, and (k) Blended SST for the CMC analysis; (l) REMSS analysis, (m) MURSST, (n) MGDSST, and (o) Blended SST for the OISST; (p) MURSST, (q) MGDSST, and (r) Blended SST for the REMSS analysis; (s) MGDSST and (t) Blended SST for the MURSST; and (u) Blended SST for the MGDSST. (a'–k') are enlarged from (a–k), respectively.

- Most of the results showed high variability in the coastal regions and low variability off-shore.

Discussion

Absence of Microwave SST

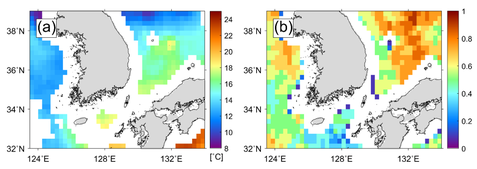

Fig. Spatial distribution of (a) sea surface temperature (SST) from the Advanced Microwave Scanning Radiometer 2 (AMSR2) on 25 April 2016 and (b) probability for AMSR2 observation for 2016.

Effect of Front

Effect of Tidal Mixing and Upwelling

Fig. Monthly variation of root-mean-squared errors (RMSE) of (a) OSTIA, (b) CMC analysis, (c) OISST, (d) REMSS analysis, (e) MURSST, (f) MGDSST, and (g) Blended SST for the in-situ measurements of each coastal wave buoy. ▶

◀ **Fig.** (a) Spatial distribution of sea surface temperature (SST) gradient using the OSTIA, and root-mean-squared errors for the (b) CMC analysis, (c) OISST, (d) REMSS analysis, (e) MURSST, (f) MGDSST, and (g) Blended SST for the OSTIA, as functions of the SST gradient. The color represents the percentage of the data to the total number in each bin.

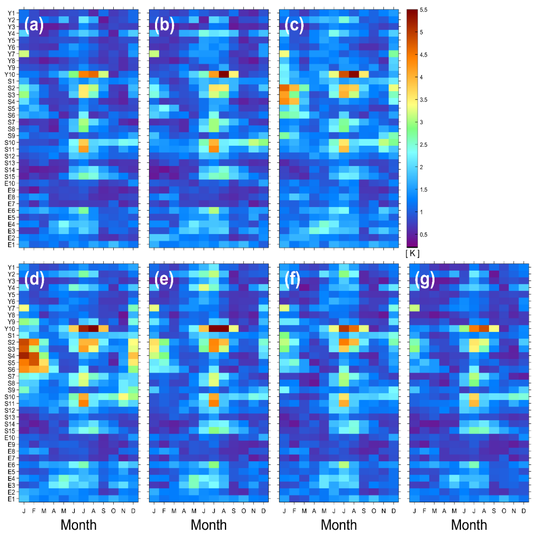

Summary and Conclusions

- Our results indicated that SST analyses had a positive bias errors ranging from 0.31 K to 0.77 K and RMSEs ranging from 1.27 K to 1.76 K, in the coastal region of the Korean Peninsula.
- Temporal scales and similarity between the in-situ temperatures and satellite-based SST database were examined using comparison of the wavelet coherence. This coherence was high (>0.8) for long periods (>180 days) and much less for short periods (<30 days).
- This study revealed the SST differences between onshore and offshore regions and addressed the importance of using as many coastal buoy measurements as possible in the production of the SST analysis database. This is particularly important for the coastal phenomena with small spatial scales, which exist over short time-scales in the coastal regions.

[**Acknowledgement**] This study was supported by the National Research Foundation of Korea (NRF), grant funded by the Korean government (MSIT) (No. 2020R1A2C2009464).